Investigation of Motor Units Activity: Comparison of Single Channel Surface EMG Deconvolution and Blind Source Separation of Multichannel Data

IEEE Access
Multidisciplinary | Rapid Review | Open Access Journal

Received 19 February 2024, accepted 13 March 2024, date of publication 21 March 2024, date of current version 27 March 2024.

Digital Object Identifier 10.1109/ACCESS.2024.3380005

APPLIED RESEARCH

Investigation of Motor Units Activity: Comparison of Single Channel Surface EMG Deconvolution and Blind Source Separation of Multichannel Data

LUCA MESIN[1], EMILIANO ROBERT[1], GENNARO BOCCIA[2], AND TAIAN VIEIRA[3]
[1]Mathematical Biology and Physiology Research Group, Department of Electronics and Telecommunications, Politecnico di Torino, 10129 Turin, Italy
[2]NeuroMuscularFunction Research Group, Department of Clinical and Biological Sciences, University of Turin, 10124 Turin, Italy
[3]LISiN, Department of Electronics and Telecommunications, Politecnico di Torino, 10129 Turin, Italy

Corresponding author: Luca Mesin (luca.mesin@polito.it)

This work involved human subjects or animals in its research. Approval of all ethical and experimental procedures and protocols was granted by the Ethical Committee of University of Torino under Application No. 510190, and performed in line with the Declaration of Helsinki.

ABSTRACT The firing instants of single motor units (MUs) can be identified by decomposing electromyograms (EMG) detected with intramuscular or grids of surface electrodes. The latter is sometimes preferred due to its larger detection volume and non-invasiveness. When the interest is in firing instants and not in investigating the activity of specific MUs, in-silico studies have shown that deconvolution of a single surface EMG is a low cost method providing reliable information. In this study, we explored this possibility by testing the experimental validity of deconvolution by comparison with decomposition of multichannel surface EMG. A single kernel deconvolution method is proposed to estimate the cumulative firings of the MUs from bipolar surface EMGs collected from the biceps brachii of 10 healthy subjects, recorded during contractions of different force levels and an endurance test. Different parameters were tested: force levels, inter-electrode distance, electrode size and location. Validity was assessed by correlating the cumulative firings (after 5-45 Hz band-pass filtering) between the proposed, deconvolution approach and the already validated, EMG decomposition. For all conditions tested, decomposition and deconvolution provided correlation coefficients of about 40%. When considering experimental signals reconstructed with the firings of decomposed MUs, markedly higher correlation values were obtained (median correlations of 90%). High correlation (about 80%) was obtained even when a signal with large interference was built by adding about 90 MU action potential trains, decomposed from different EMGs of our dataset with same contraction levels. Analysis of residual root mean squared error (median across tests of about 40% and 15% for decomposition and deconvolution, respectively) together with the good estimation on reconstructed signals with high interference suggest that deconvolution may identify additional contributions that are not explained by decomposition. This additional information provided by deconvolution may justify in part the discrepancy when comparing the outputs of the two methods applied to the original signals. The cumulative firing instants associated with action potentials can be accurately estimated with the deconvolution of a single bipolar surface EMG.

INDEX TERMS Surface EMG, decomposition, deconvolution.

I. INTRODUCTION

Investigating the mechanisms governing the control of motor units (MU) is important in many fields. For example, MUs firing properties have been shown to change with training [1],

The associate editor coordinating the review of this manuscript and approving it for publication was Hasan S. Mir.

force [2], fatigue [3], [4], pain [5] and pathology [6]. Indeed, the cumulative spike trains of the MUs reflect the overall drive of the muscle of interest and the extraction of the information they include from the entire EMG provided useful insights into muscular central control [7], [8], [9], [10]. Moreover, the study of recruitment and rate coding of MUs has broadened our knowledge on cortico-muscular synchronization [11], common drive [12] or common synaptic input [13], intra-muscle and inter-muscles coherence [14], [15] and muscle synergies [16], [17].

Advanced processing methods allow to decompose the interference EMG into the contribution of single MUs [18]. The possibility of studying single MUs is useful to extract information on muscle activity, e.g., to improve the estimation of muscle force [19], [20], contraction velocity [21], joint angle [22] and in the control of a myoelectric prosthesis [23], [24], [25], [26]. Two main approaches have been conducted to decode single MUs activations: decomposition of intramuscular EMG [27] and decomposition of surface EMG detected with grids of electrodes [28]. Being non-invasive, this high-density approach [29], [30], [31] has garnered the interest of both clinical and technical users [32], [33]. However, notwithstanding the important insights into the neuromuscular control strategies obtained with decomposition of high-density EMGs [18], this approach requires using grids of electrodes with dedicated amplifiers and computationally intensive processing techniques.

In spite of the limited spatial sampling, circumstances often impose the use of the traditional bipolar montage (also called single-differential, SD). Bipolar EMGs are easy to use, minimally restrain movements and require small resources of memory and power, likely explaining its overwhelming popularity in applied fields (e.g., ergonomics [34], sport science [35], gait analysis [36] and clinics [37]). In contrast to high-density EMGs, bipolar recordings offer little, if any, possibility of identifying single MUs: the temporal summation of action potentials of different MUs is unlikely resolved for a single detection point. Nevertheless, if interest lies in the instants at which the target muscle has been excited, regardless of where depolarization took place within the muscle, the process of labelling the excitation instants[1] according to specific MUs is not required. For example, the energy of frequencies up to about 40 Hz was suggested to reflect the average firing rate of MUs recruited during submaximal, voluntary contractions [7], [8]. In order to extend the range of applicability to higher contraction levels, different methods were proposed, including rectification [38] (which was questioned due to its non-linear nature [9]) and identification of non-propagating components [10], [39] (which requires monopolar recordings).

The possibility of collectively assessing the firing rate of populations of MUs from a single bipolar EMG motivated the emergence of a deconvolution method, sought for identifying the cumulative firing instants of whichever source could be excited [40], [41]. While the application of deconvolution to simulated EMGs has shown promising outcomes, similarly encouraging results on experimental EMGs are limited to the preliminary observation that better myoelectric control may be obtained with EMG deconvolution rather than with original EMGs [42]. An experimental validation of EMG deconvolution is thus warranted before it can be considered for the identification of excitation instants from experimental bipolar EMGs.

This study aims therefore at validating the deconvolution method applied to a bipolar EMG against the gold standard for MU identification in surface EMG: decomposition of high-density EMG. We specifically assess whether the deconvolution method identifies the firing instants of biceps brachii MUs decomposed from experimental EMGs with an automated, validated procedure. Focus is placed on the firing instants, regardless of their sources. The following workflow is followed.

1. Recording of surface EMG during contractions at different force levels and endurance from a 2D electrode grid in monopolar configuration.
2. Decomposition of recorded EMGs, using the information from the entire electrode grid.
3. Computation of bipolar signals from the recorded high-density data, with different inter-electrode distance, electrode size and location.
4. Deconvolution of single bipolar EMGs.
5. Comparison of information obtained from single-channel deconvolution and decomposition of the high-density signals, both in terms of average MU discharges estimated and signal power explained.
6. Generation of high interference signals as sums of MU action potential (MUAP) trains identified by decomposition to test deconvolution on challenging data with known firing statistics.

Our results suggest that deconvolution may provide a physiologically plausible estimation of the cumulative trains of excitation instants from a single bipolar EMG.

After this introduction, the manuscript proceeds with a Methods section, describing the experimental recordings, the processing methods (namely, decomposition and deconvolution) and the tests for comparison. Then, the Results and Discussion sections show and interpret (respectively) the outcomes of our research. A final summary of our work is given in the Conclusions section.

II. METHODS

A. EXPERIMENTAL PROTOCOL

Ten healthy males (mean age 25 years, range 22-28 years) participated to the experiments. None reported any previous musculoskeletal pathologies. All subjects provided written, informed consent prior to undertaking the experiment. Data were recorded in accordance with the Declaration of Helsinki.

[1] Excitation instants is used here to explicitly distinguish trains of impulses corresponding to the firing instants of specific MUs from the sum of all impulses from all active MUs (cumulative firing instants).

The study was approved by the Ethical Committee of University of Torino (approval no: 510190).

EMG signals were acquired from the biceps brachii during isometric contractions at different force levels. Before the acquisition, participants were asked to perform two maximal voluntary contractions (MVC), resting two minutes in-between. Then, they performed two isometric contractions at different force levels: 10% MVC, 30% MVC, 50% MVC and 70% MVC resting 2 minutes in-between. Participants were asked to maintain a constant force for 15 s during the 70% MVC trials and for 20 s otherwise, while provided with visual force feedback overlaid on a trapezoidal, reference signal. The trapezoidal profile imposed reaching with a fixed rate of 10% MVC/s the submaximal, target plateau (to be kept for 15 or 20 s, as detailed above) and then come back to rest (again with a rate of 10% MVC/s). Finally, the subject performed a fatiguing isometric contraction to exhaustion with a force level of 60% MVC. The test ended when the subject was unable to maintain the force over 90% of the target level for 3 s.

Figure 1 shows the experimental setup.

B. MEASUREMENTS

EMGs were acquired in monopolar configuration with a 2D grid of 64 electrodes (13 × 5; one electrode missing on the proximo-lateral edge; 8 mm interelectrode distance (IED)). The electrode grid was placed on the biceps brachii and the reference electrode on the acromion, after carefully cleaning the skin with abrasive paste. The grid was secured to the skin with adhesive pad, which holes in correspondence of electrodes were filled with conductive paste. The five columns of the grid of electrodes were aligned parallel to the muscle fibers and the grid was centered over the muscle bulge. Signals were band-pass filtered (0.7-500 Hz), amplified (gain 150), and then sampled at 2048 Hz with a 16 bit A/D converter (Quattrocento EMG amplifier, OTBioelettronica, Turin, Italy).

C. SIGNAL PROCESSING

Data were first pre-processed with a zero-lag, band-pass filter (5)-350 Hz; 4th order Butterworth). Then, the firing patterns of single MUs were extracted from monopolar EMGs using an automated and validated decomposition algorithm [30], [31]. The output was used as reference to test the deconvolution algorithm, which was applied to single bipolar EMGs. Descriptions of the processing methods and of the tests are provided below.

1) DECOMPOSITION OF MULTICHANNEL SURFACE EMG

We used the algorithm DEMUSE to decompose the recorded EMGs into constituent MUAP trains [30], [31]. The method was previously validated [43] and tested in different applications [44].

We can write the interference EMG as the asynchronous summation of different MUAPs

$$s_C(t) = \sum_{m=1}^{N} \sum_{j=1}^{J_m} M_{C,m}(t - \tau_{mj}) + n_C(t) \quad (1)$$

where $s_C(t)$ is the monopolar EMG detected by the electrode C, N is the number of active MUs, $M_{C,m}$ is the action potential from the m^{th} MU, firing J_m times, τ_{mj} is the j^{th} time in which the m^{th} MU fired and $n_C(t)$ is an additive noise (notice that variations of MUAP shapes, e.g., induced by fatigue, have been neglected). Decomposition identifies the firing pattern of different MUs using the Convolution Kernel Compensation method [30], which compensates different MUAP shapes and reconstructs the pulse trains directly. After estimating the firing patterns of different MUs, the corresponding MUAP of each MU detected at each electrode location can be retrieved by averaging. This allows for the spatio-temporal characterization of single MUs, providing information on their discharge properties [1], [2], [3], [4], [5], [6], as well as of the distribution of their fibers within the muscle [45], [46]. Moreover, the identified MUAP trains can be summed to build an estimation of the original signal (thus, allowing to evaluate the percentage amount of the original data which was decoded by the algorithm).

Decomposed signals were used to estimate the cumulative firing that could be extracted from the single SD channel used for deconvolution, as described below.

2) SINGLE CHANNEL DECONVOLUTION

The deconvolution of bipolar EMGs has been introduced in [40] (to which the reader can refer for details). A short introduction to the method is here provided.

Consider an SD channel $s(t) = s_{C_1}(t) - s_{C_2}(t)$, defined as the difference between the monopolar signals from channels C_1 and C_2. In this study, it was defined by selecting electrodes beyond the most distal innervation zone (IZ) with different IEDs, or over it and the distal tendon in the case of the test of belly tendon configuration (see below the detailed list of tests). From Equation (1), we obtain the considered SD signal as

$$s(t) = \sum_{m=1}^{N} M_m(t) * F_m(t) + n(t) \quad (2)$$

where $M_m(t) = M_{C_1,m}(t) - M_{C_2,m}(t)$ is the m^{th} MUAP in SD configuration, $*$ indicates the convolution operator, $F_m(t) = \sum_{j=1}^{J_m} \delta(t - \tau_{mj})$ is the firing pattern of the m^{th} MU and $n(t) = n_{C_1}(t) - n_{C_2}(t)$ is the additive noise.

A single kernel is used to approximate the waveforms of different MUAPs, obtaining the following approximation

$$s(t) \approx K(t) * f(t) \quad (3)$$

where $K(t)$ is the kernel and $f(t) = \sum_{m=1}^{N} \sum_{j=1}^{J_m} A_m \delta(t - \tau_{mj})$ the estimated cumulative firing pattern, representing the firings

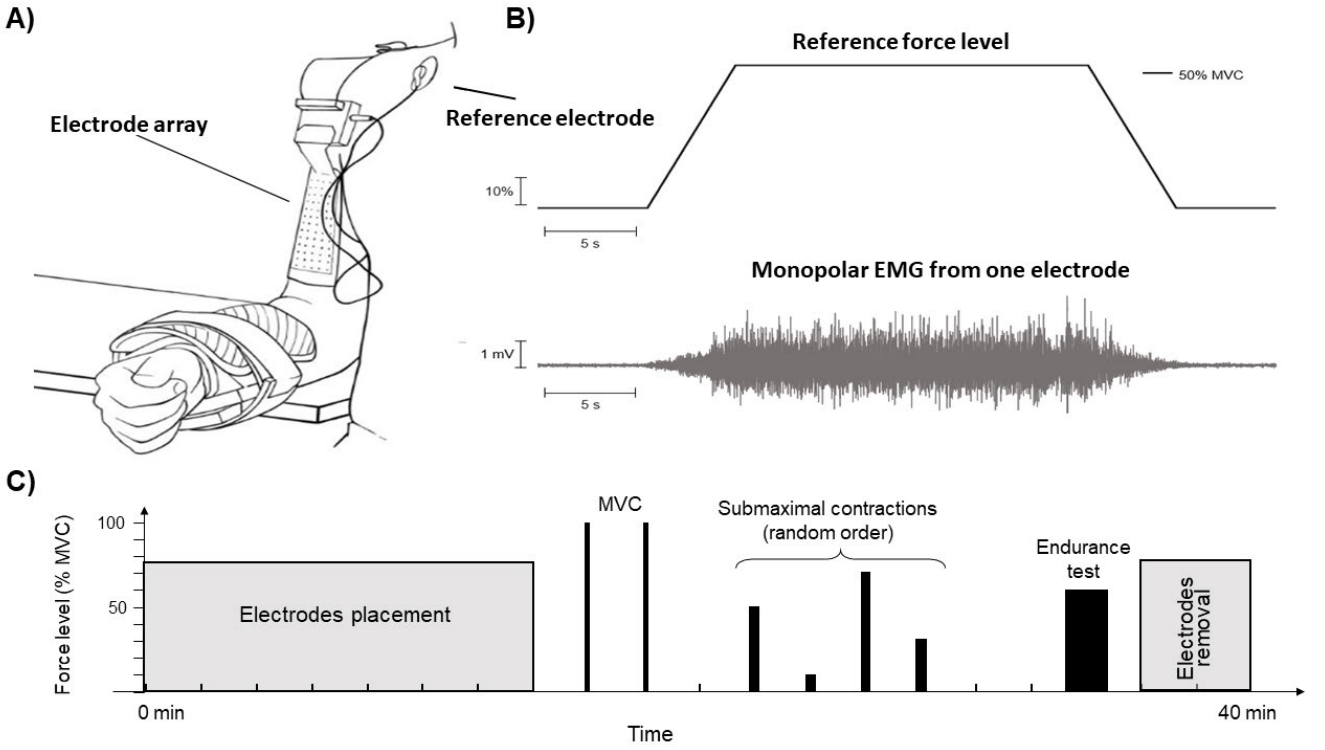

FIGURE 1. Experimental setup. A) Representation of the experimental custom-made brace and the electrode array placed on the biceps brachii of the subject. B) Example of trapezoidal visual force feedback and single monopolar EMG recorded during the contraction. C) Representation of the experimental protocol.

of all active MUs, weighted by the amplitudes $\{A_m\}_{m=1}^{N}$ of their MUAPs as they are recorded by the considered pair of electrodes [40]. The presence of noise and the shape differences among MUAPs of different MUs makes the model only an approximation. However, simulation tests revealed that this model may provide reliable information on the biophysics underlying the generation of the recorded signal [40].

The kernel was written as the first derivative of a Gaussian function, as this shape resembles that of MUAPs recorded in SD configuration [47] (the adaptation of the shape of the kernel to the signal could be an interesting development, left for future investigation). The power spectral density (PSD) of the first derivative of a Gaussian function is

$$\dot{G}(t) = \frac{d}{dt}\frac{e^{-\frac{t^2}{2\sigma^2}}}{\sqrt{2\pi\sigma^2}} \quad \rightarrow \quad F[\dot{G}(t)] = j2\pi f e^{-2\pi^2 f^2 \sigma^2}$$
$$\rightarrow \quad PSD = |F[\dot{G}(t)]|^2 = 4\pi^2 f^2 e^{-4\pi^2 f^2 \sigma^2} \tag{4}$$

where F indicates the Fourier transform. In order to estimate the optimal variance σ^2, the slope of the following 1D curve was computed

$$\Gamma(f^2) = \left(f^2, \log\frac{PSD}{4\pi^2 f^2}\right) \tag{5}$$

for the PSD of the specific EMG to be processed, considering the frequency range in which most of the power is found, i.e., in $(F_{Med} - F_{std},\ F_{Med} + 2F_{std})$, where F_{Med} is the median frequency and F_{std} the standard deviation of the PSD (previous tests showed that this range provides stable results [41]).

Given the kernel, the cumulative firing pattern $f(t)$ in Equation (3) was computed by deconvolution. As preliminary step, the following energetic functional with Tykonov regularization [48] was considered

$$argmin_{\hat{f}(t)} \left\| s(t) - K(t) * \hat{f}(t) \right\|_2^2 + \alpha \left\| \hat{f}(t) \right\|_2^2 \tag{6}$$

where α is the regularization parameter. The problem was discretized writing convolution as the multiplication of the unknown sampled cumulative firing with a matrix as in [40], [49], and [50]

$$AX \approx b \tag{7}$$

where A is a lower triangular Toeplitz matrix collecting the samples of the kernel, $b = \{b_i\} = \{s(t_i)\}$ is the vector of recorded data samples and X the unknown time distribution of firings.

After this sampling, the functional to be minimized in (6) is

$$\|AX - b\|^2 + \alpha\|X\|^2 = \left\| \begin{bmatrix} A \\ \sqrt{\alpha} I \end{bmatrix} X - \begin{bmatrix} b \\ 0 \end{bmatrix} \right\|^2 = \|BX - c\|^2 \tag{8}$$

where

$$B = \begin{bmatrix} A \\ \sqrt{\alpha} I \end{bmatrix}, \qquad c = \begin{bmatrix} b \\ 0 \end{bmatrix} \tag{9}$$

with solution

$$X = (B^T B)^{-1} B^T b = (A^T A + \alpha I)^{-1} A^T b \tag{10}$$

The 1% of the maximum eigenvalue of $A^T A$ was chosen as regularization parameter α, so as to limit the condition number of the matrix $A^T A + \alpha I$ to 100 (this choice was supported by a fine tuning performed in previous studies, based on simulations [40], [41]).

In order to get a solution more sparse (thus, better resembling a firing pattern) and robust to outliers [51], the L_1 norm was used instead of the L_2. The solution was obtained by the iterative reweighted least square (IRLS) method [48], starting from the solution of the L_2 problem and making 10 iterations to minimize the following error functional

$$\left\| \begin{bmatrix} A \\ \sqrt{\alpha} I \end{bmatrix} X - \begin{bmatrix} b \\ 0 \end{bmatrix} \right\|_{L_1} = \\ = \left\| W^T \cdot \left(\begin{bmatrix} A \\ \sqrt{\alpha} I \end{bmatrix} X - \begin{bmatrix} b \\ 0 \end{bmatrix} \right) \right\|_{L_2}^2 \tag{11}$$

where W, initialized as the identity and updated for each iteration, should be equal to the reciprocal of the square root of the absolute error at convergence. The estimated solution was also imposed to be positive at each iteration, by assigning zero to negative values.

Splitting properly the signal in short overlapping epochs, it is possible to decrease the computational cost, getting virtually the output of the algorithm in real time [40] (even if offline processing was considered in this work).

3) TESTS

Individual SD EMGs from the grid were chosen to be processed by the deconvolution algorithm. The choice was based on visual analysis of the signals collected with the electrode grid. The selected channel was chosen beyond the most distal IZ, in order to consider a region in which all action potentials propagated in the same direction.

The decomposition algorithm provided firing instants of different labelled MUs. Their corresponding action potentials were estimated for each electrode by spike triggered averaging. Then, by convolution of the firing patterns with the corresponding action potential, the MUAP trains were obtained.

Given the decomposition of the EMGs into MUAP trains, tests of deconvolution were performed either on the original data from the selected channel or on reconstructed signals, defined as the sum of the MUAP trains detected by EMG decomposition. Below is a list of all tests performed and their rationale.

1) Spatial filter selectivity: EMGs with different IEDs, ranging from 8 mm to 32 mm. Rationale: the effect of the selectivity of the bipolar spatial filter on deconvolution is tested.
2) Belly-tendon sampling: two large square electrodes were simulated, summing the potential recorded by different electrodes,[2] displaced over regions of dimensions 2 × 2 (IEDs, corresponding to a covered surface of 8 × 8 mm^2, i.e., 0.64 cm^2), 3 × 3 (2.56 cm^2) and 4 × 4 (5.76 cm^2); the two large square electrodes were placed over the IZ and the most distal tendon, respectively. Rationale: using large electrodes in belly-tendon configuration is a common practice in some clinical settings [49], [50], so that exploring the value of deconvolution in this scenario can be important.
3) The solutions provided by the deconvolution algorithm were compared for different columns of the grid (with the aim of testing the sensitivity of the output of the algorithm to a displacement of the detection channel in the direction transverse to the muscle fibers). The algorithm was applied to SD signals characterized by different IEDs, i.e., 8 mm, 16 mm and 24 mm. Rationale: repeatability of information extraction is crucial in any biomedical application. When repeating a measurement of surface EMG on the same subject, it is possible to identify some points of repere (e.g., some anatomical details, including the location of IZ and tendons), but a displacement in direction transverse to the muscle fibers is difficult to avoid. This test is aimed to reveal the sensitivity of deconvolution in case of transverse displacements and as a function of the selectivity of the filter (i.e., the IED of the bipolar detection).
4) Test on signals of high interference, simulated by adding many experimental MUAP trains: five interference signals in increasing order of complexity were constructed, by summing the trains of MUAPs detected by decomposing different data. White Gaussian noise of different power has been added to obtain signals with different SNRs, i.e., 20 dB, 10 dB and 5 dB. Rationale: surface EMGs with high interference are the most difficult to be processed and even the decomposition algorithm can have problems in decoding all information included. Using signals obtained by adding experimental MUAPs is a way to test deconvolution on high interference data having a reference output.

D. COMPARISON OF CUMULATIVE SPIKES FROM DECOMPOSITION AND DECONVOLUTION

We compared the cumulative weighted firings (CWF) of decomposition and the output of deconvolution. To build the CWF, the firing patterns of the MUs identified by decomposition were weighted by the root mean squared (RMS) of their MUAPs (as detected by the SD channel processed by deconvolution), estimated by spike triggered averaging, and summed up. The obtained time series were filtered between 5-45 Hz. Beyond this frequency range,

[2]Notice that a metallization imposes constant potential under it, thus affecting the signal that it is sensing. Thus, summing the potentials from different electrodes is only an approximation of the recording obtained by a large electrode covering an area sampled by those electrodes.

it is not reasonable that deconvolution can provide reliable estimations. However, notice that information about MU firing rate is included in such a range. The two filtered time series (obtained respectively by decomposition and deconvolution) were compared by the correlation coefficient, which was explored by statistical analysis.

To correct the skewness in the data distribution, the statistics were performed on log-transformed data. Then the Shapiro-Wilk tests confirmed normality of the distributions. Thus, to test our experimental questions we performed a series of repeated measure ANOVAs with the following factors: type of signal (binary variable indicating either raw data or reconstructed), force level (5 levels: 10%, 30%, 50%, 70% of MVC and 60% for the endurance test), size of electrodes (3 levels: 2 × 2, 3 × 3, 4 × 4), IED (3 levels: 8, 16 and 24 mm), and transverse electrode distance (3 levels: 8, 16 and 24 mm). The Greenhouse-Geisser correction was adopted when sphericity was violated. The effect size was determined using partial η^2.

III. RESULTS

An example of the processing procedure is shown in Figure 2. The monopolar EMGs from the entire grid of electrodes were decomposed. The CWF estimated by decomposition of monopolar EMGs and the output of deconvolution algorithm, applied to a single, SD EMG, were compared. The correlation coefficient of these time series was computed.

The distributions of correlation coefficients between CWFs from decomposition and single channel deconvolution (both filtered in the range 5-45 Hz) are shown in Figure 3, considering a single SD EMG with 8 mm IED, for each force level and the endurance contraction. Both original and reconstructed signals were considered. There was a large significant difference between original and reconstructed signals ($F(1,9) = 173.8$, $P < 0.001$; $\eta^2 = 0.951$), while there were no differences between force levels ($F(1.9,17.1) = 2.3$, $P = 0.131$; $\eta^2 = 0.204$).

The distributions of correlation coefficients of CWF from decomposition and deconvolution are shown in Figure 4, considering a belly-tendon detection. Using larger electrodes (simulated by summing the potentials from more electrodes in the grid), the detection volume slightly increases and the signal becomes smoother. However, the correlation between the outputs of decomposition and deconvolution did not depend on the electrode size ($F(2,18) = 0.1$, $P = 0.815$, $\eta^2 = 0.009$).

Figure 5 shows the distributions of the correlation coefficients computed between CWFs estimated by decomposition and deconvolution, considering different IEDs and thus different detection volumes. There was a significant interaction between input signal and IED ($F(1.3,11.7) = 9.0$, $P = 0.008$; $\eta^2 = 0.503$). The correlation coefficients increased with IED, but the increment was larger for original than for reconstructed data. However, the correlation coefficients remained higher for reconstructed than original signals ($F(1,9) = 90.0$, $P < 0.001$; $\eta^2 = 0.909$).

The sensitivity of deconvolution when applied to different channels, displaced in direction transverse to muscle fibers, is reported in Figure 6. Correlation of estimations increased with the IED of the channels ($F(1.3,12.1) = 21.1$, $P < 0.001$; $\eta^2 = 0.702$) and decreased with the distance among channels ($F(1,10) = 5.6$, $P = 0.036$; $\eta^2 = 0.387$).

Figure 7 shows a test on interference data built by summing more MUAP trains resulting from the decomposition of high-density EMGs (the number of MUAP trains summed up is indicated in Figure 7A). To increase the degree of interference in the resulting SD EMG, MUAP trains decomposed from different subjects were summed. Different levels of white Gaussian noise have also been included, to further stress the algorithm. Correlation of actual CWF and deconvolution was quite high, with a decrement when increasing the number of MUAP trains considered, but still getting values around 80% with the largest interference and minimum SNR.

As shown in Figure 8, the trains of firings obtained with decomposition and deconvolution do not allow to reconstruct the original signal to equal extents. The ability of deconvolution to extract a greater number of sources when compared with decomposition is evident when overlaying the MUAPs on the original signal (Figure 8A-B). Group results confirm that, regardless of the contraction intensity, and thus of the degree of interference, the residual energy after removing the estimated from the original signal is significantly lower when deconvoluting the target SD signal than decomposing the high-density EMGs (Figure 8C; main effect of contraction level: $F(1,9) = 99.8$, $P < 0.001$; $\eta^2 = 0.917$). Deconvolution was also less sensitive to the contraction level than decomposition (interaction effect: $F(1.2, 8.5) = 35.4$, $P < 0.001$; $\eta^2 = 0.835$).

IV. DISCUSSION

The study of MU recruitment and rate coding has advanced our understanding in various applications, e.g., muscle force [19], [20], speed of contraction [21], joint angle [22], fatigue [52] and accuracy in the control of myoelectric prostheses [23], [24]. Various methods have been used to extract this information, by decomposition of interference EMG into MUAP trains [25], [26]. However, due to the complexity of the acquisition system and the high computational cost, the use of these methods in practical applications can be inconvenient. Some recent approaches proposed even fast processing [25], [26], but still are not suited to single bipolar EMGs.

An innovative method was therefore proposed for the estimation of the cumulative spike trains of MUs by processing a single SD channel [40]. The new algorithm, based on a single kernel deconvolution technique, is able to roughly reconstruct the cumulative firing instants of the active MUs. The simulation tests, previously conducted to evaluate the accuracy and precision in the reconstruction, have produced promising results [40]. Therefore, here we evaluated the performance of the deconvolution algorithm

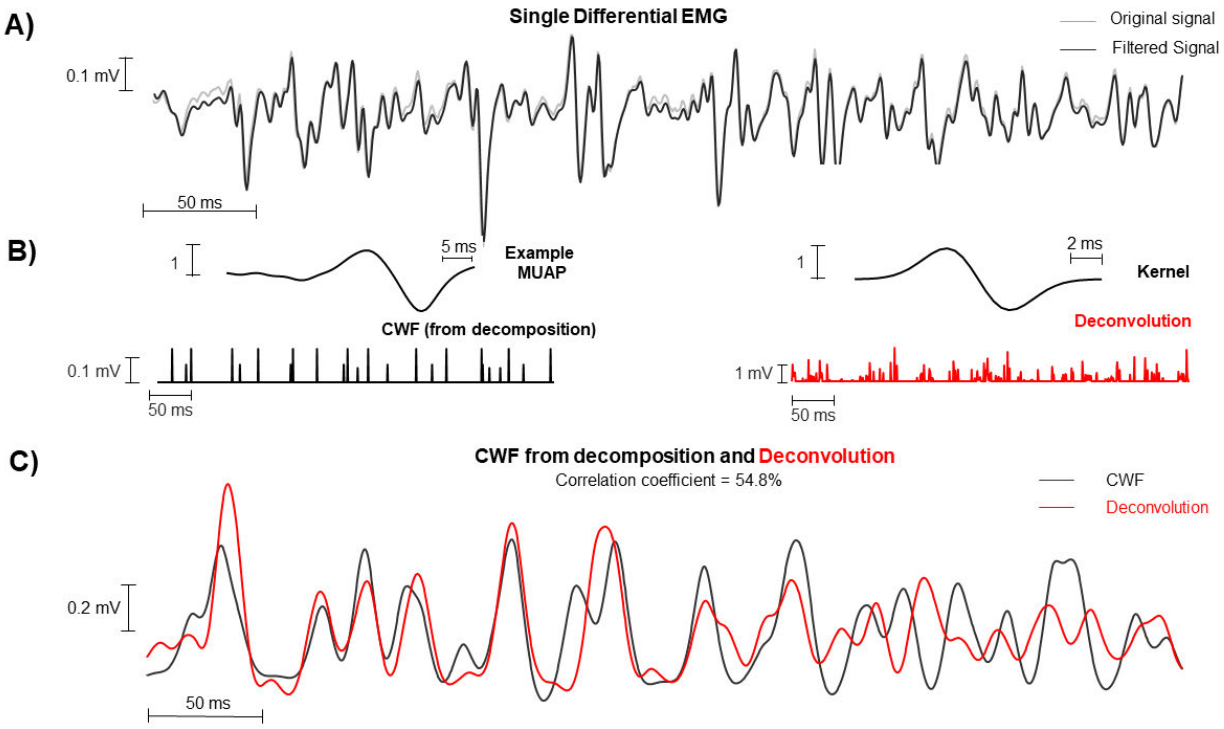

FIGURE 2. Example of processing of an epoch of EMG. A) Original and pre-processed signal (i.e., filtered in the range 5-350 Hz). Single differential (SD) channel manually selected from EMGs detected with a two-dimensional grid of electrodes. B) Decomposition and deconvolution of the same signal (a single MUAP from decomposition is shown, together with the cumulative weighted firings - CWF - obtained considering all MUAPs decomposed). C) Outputs of decomposition and deconvolution, filtered in the range 5-45 Hz, with indication of their correlation.

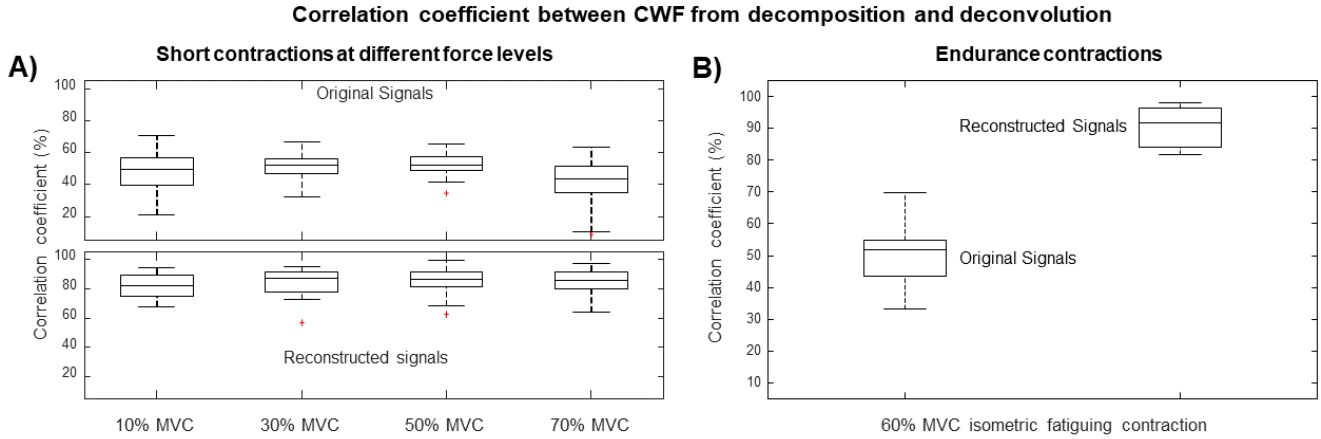

FIGURE 3. Distributions of correlation coefficients between CWF estimated by decomposition and single channel deconvolution, applied to both original and reconstructed signals for 8 mm IED. A) Submaximal, trapezoidal contractions. B) Endurance contraction.

through experimental tests in order to understand the effective capacity and applicability in the field. The algorithm was applied to single channels taken from experimental EMGs recorded through a 2D grid of 64 electrodes in monopolar configuration, from the brachial biceps of 10 healthy subjects during isometric contractions at different force levels and in a fatiguing test. The output of single channel deconvolution was compared to that of a validated decomposition algorithm [30], [31]applied to signals recorded from the entire electrode grid (Figure 2).

Before discussing results arising from deconvolution and decomposition methods, a technical note is warranted here. Full experimental validation of our deconvolution method would require the identification of firings of all MUs located within the detection volume of the bipolar EMG we considered here. Experimentally, we are not aware

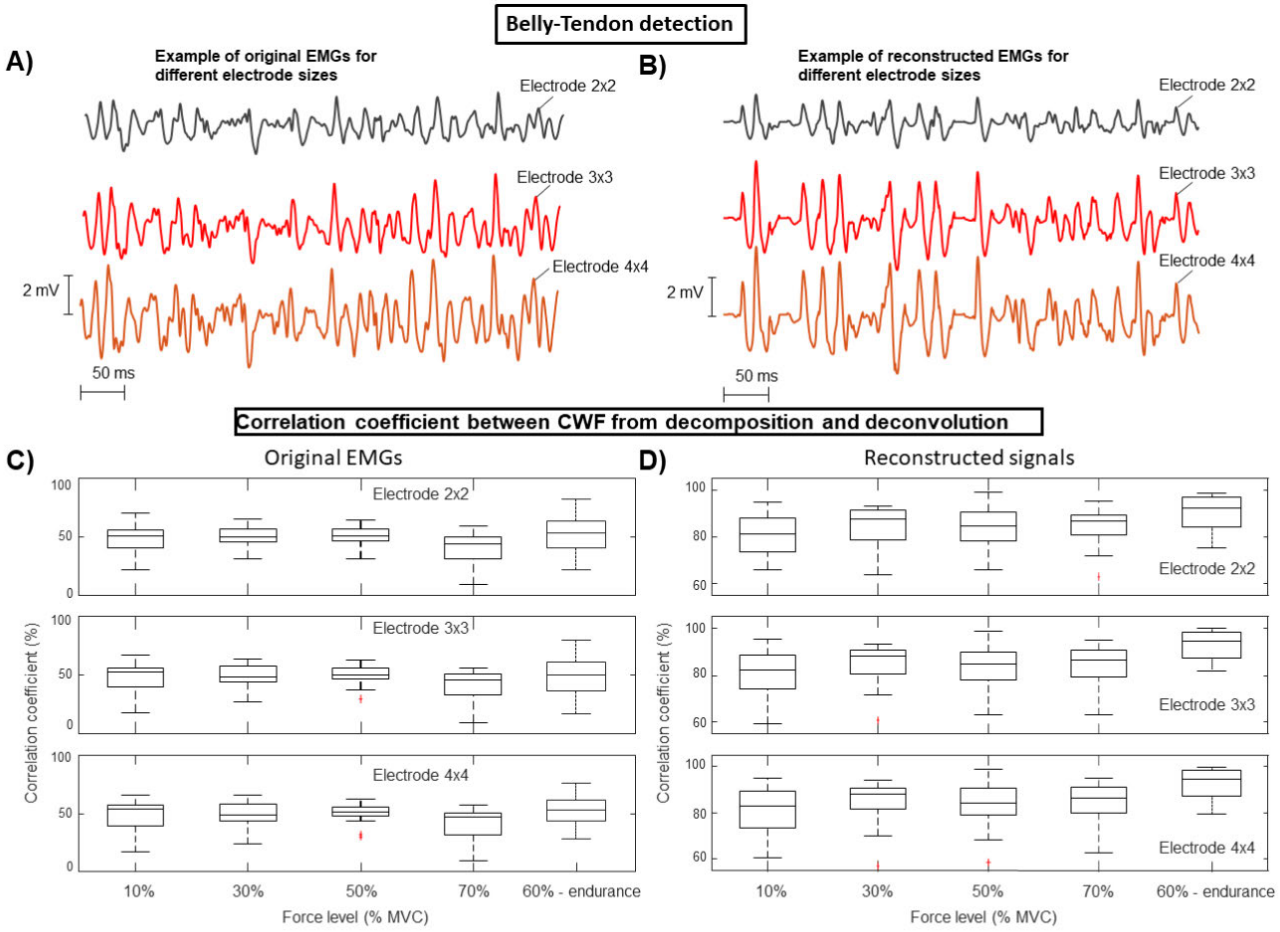

FIGURE 4. Distributions of correlation coefficients between CWF estimated by decomposition and deconvolution, applied to a single channel in belly-tendon configuration with different electrode sizes: square electrodes of size 2 × 2 (IEDs), 3 × 3, 4 × 4. Original and reconstructed EMGs were considered in A-C-E) and B-D-F), respectively. A-B) Examples of signals (same EMG epoch, either original or reconstructed). C-D) Distributions of correlation coefficients in box and whisker plots considering submaximal, trapezoidal contractions. E-F) Distributions of correlation coefficients in the case of 60% MVC endurance contractions.

of a gold standard against which we could assess our deconvolution method. Intramuscular EMG, albeit being the clinical reference for assessing neuromuscular control, would provide a limited number of MUs.[3] Owing to the multiple detection points, each positing a larger detection volume in relation to a single intramuscular recording, the decomposition of high-density EMGs would be expected to disclose the greatest number of MUs. Different algorithms for decomposition of surface EMGs have been developed [29], [30], [31], [54]. We selected one specifically tailored for decomposition of high-density surface EMG, likely yielding the greatest number of MUs for creating the cumulative spike train.

The tests were conducted both on the original signals and on those reconstructed from decomposition estimates (Figure 3). Moreover, we considered both recordings at different effort levels and an endurance contraction, obtaining similar performances: in fact, the algorithm adapts to the signal (thus compensating the average effect of the volume conductor on the sources) and its performance is not directly impaired by factors like the number of active MUs, their specific timing of activation or their progressive fatigue. Many conditions have been considered, extracting different SD channels from the 2D grid of electrodes and obtaining quite stable indication across different dimensions of the electrodes (Figure 4) and IEDs (Figure 5). Specifically, a detection in belly-tendon configuration was considered (Figure 4), showing stable results across different electrode sizes. Notice that, by increasing the size of the electrodes (here simulated by summing the signals from more physical electrodes), the detection volume increases, thus representing the activity of a larger portion of the investigated muscle, with more contributions included to the recorded interference signal. The correlation coefficients of estimations obtained

[3]There is also an advanced high-density intramuscular electrode system that can identify the activity of a large number of MUs [53]. Its use to validate deconvolution is an interesting future perspective.

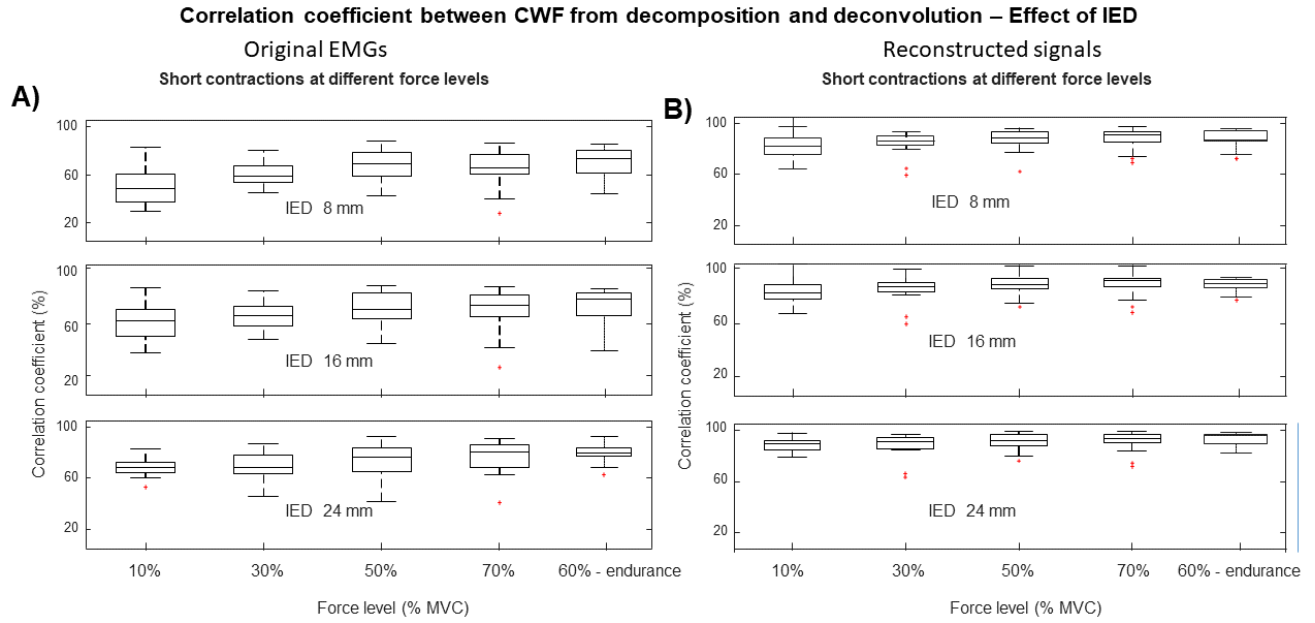

FIGURE 5. Effect of IED on the correlation coefficients between CWF estimated by decomposition and deconvolution. Original and reconstructed EMGs were considered in A-C) and B-D), respectively. A-B) Submaximal, trapezoidal contractions. C-D) 60% MVC endurance contraction.

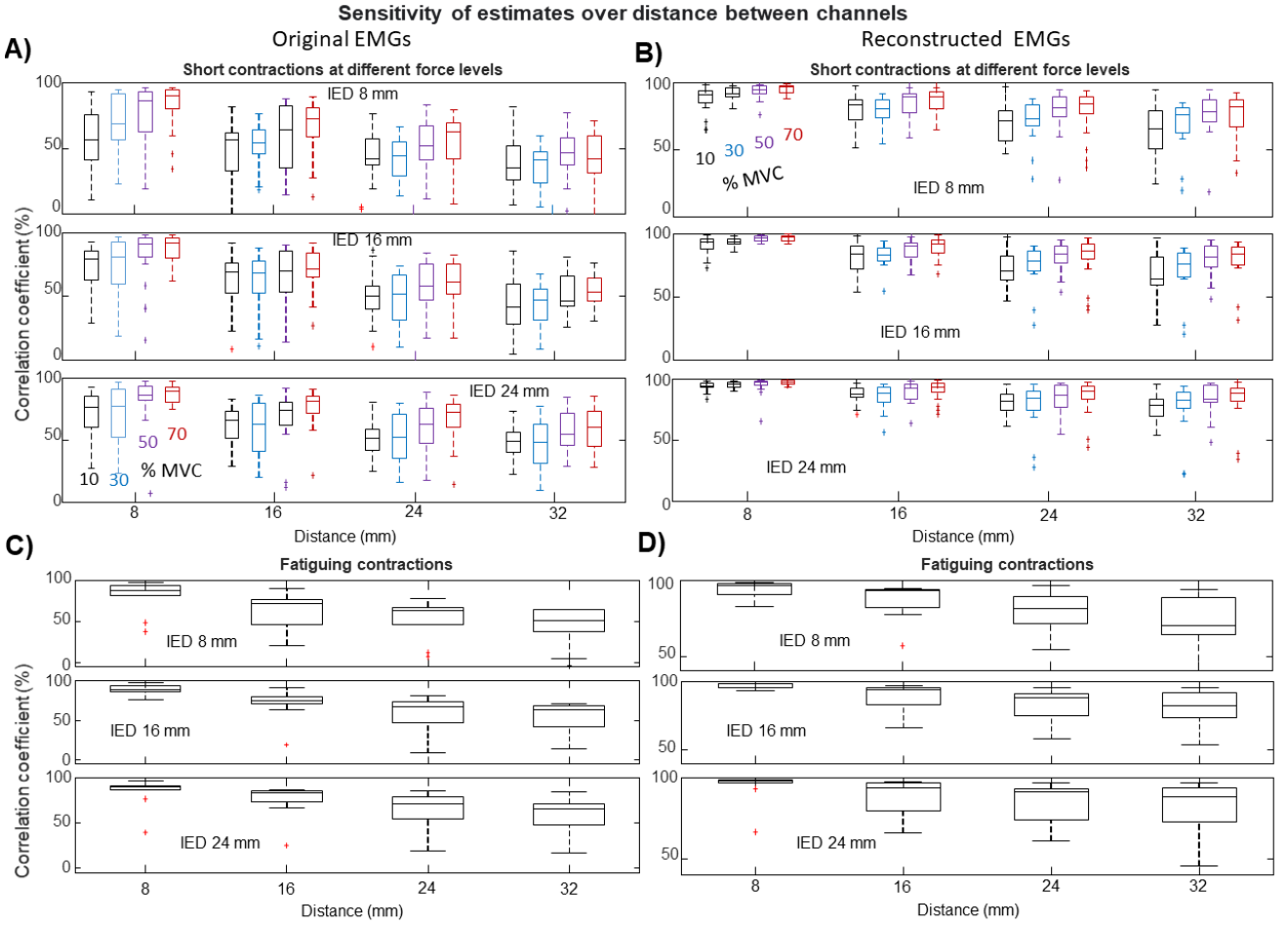

FIGURE 6. Effect of electrode transverse location on the correlation coefficient between CWFs estimated by deconvolution. The deconvolutions of the signals from the first column of the electrode grid were compared to those of the signals from other columns, with different transverse distances. Different IEDs were considered. Both A-C) original and B-D) reconstructed EMGs have been processed. A-B) Submaximal, trapezoidal contractions. C-D) Endurance test.

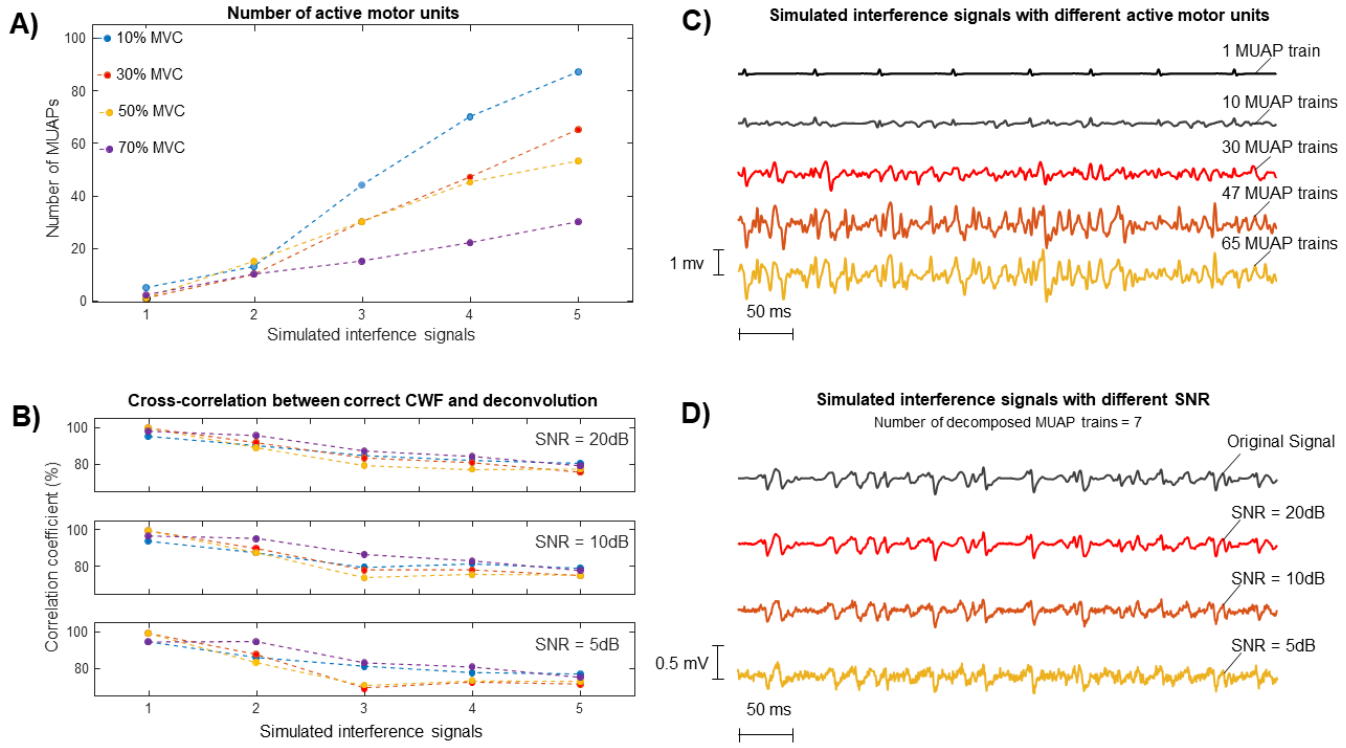

FIGURE 7. Testing of the effect of the degree of interference EMGs. Signals were obtained summing MUAP trains decomposed from different subjects at the same force levels. A different number of MUAP trains was summed, to test the effect of the degree of interference. Moreover, white Gaussian noise was added, with different SNR. A) Number of motor units that make up the five interference signals, extracted from data recorded at different force levels. B) Correlation of actual and estimated CWF (both filtered in the range 5-45 Hz) obtained by processing five simulated interference signals for each test with an increasing number of motor units (indicated in A). White Gaussian noise was also added to the simulated interference signals, with different SNRs. C) Examples of signals obtained summing a different number of trains of motor unit action potentials (MUAP). D) Example of a signal corrupted by different levels of white Gaussian noise.

from the original signals were about 50%, but their median values were over 80% when applied to reconstructed signals. Belly-tendon configuration is used in many clinical scenarios [49], [50] [55], indicating possible future applications of the algorithm.

The detection volume is also increased when considering a bipolar signal with larger IED: Figure 5 indicates a small (but significant) increase of the match between the outputs of decomposition and deconvolution in this condition, both considering original and reconstructed data. Keeping small the electrodes and enlarging only the IED in the direction of the muscle fibers, the detection volume goes deeper, without extending much in the transverse direction, as done with the belly-tendon simulation above-mentioned. This way, the interference (and consequently also phase cancellations) is expected to increase less, which is possibly the reason why enlarging the IED has more beneficial effects on output reliability (in terms of matching with the output of decomposition) than increasing electrode size, even if in both cases the detection volume increases.

Furthermore, similar results were obtained by deconvolution when displacing the SD detection channel in transverse direction (Figure 6), with higher correlation coefficients with greater IED, due to the lower selectivity and thus larger detection volume (e.g., more than 80% of median correlation, considering an IED of 24 mm and a displacement of 16 mm). This suggests that the estimations are not much sensitive on the specific location of the detection channel, mostly if a great IED is used. Thus, comparison of recordings taken in different days on the same subject (thus, expecting some displacement of the detection channel) could be feasible.

As correlation coefficients of the outputs of decomposition and deconvolution is really high only if signals are reconstructed and not using the original data, there could be some concern about the performance of deconvolution when managing data with large interference. Figure 7 shows a test on interference data obtained by summing more MUAP trains extracted from different recordings. Indeed, as only the activity of few MUs could be recovered by decomposition of a single acquisition, this was the only way to obtain complex EMGs with great interference. Obviously, recovering MU activity is more difficult when many contributions are superimposed, as phase cancellation is more important, so that some of the information is erased. However, performances of deconvolution with these signals show high correlation with the CWF (even when including additional noise), suggesting that part of the discrepancy between deconvolution and the CWF from decomposition was due to the signal power not explained by the latter. Indeed, decomposition can recover a smaller portion of the energy included in the original signal

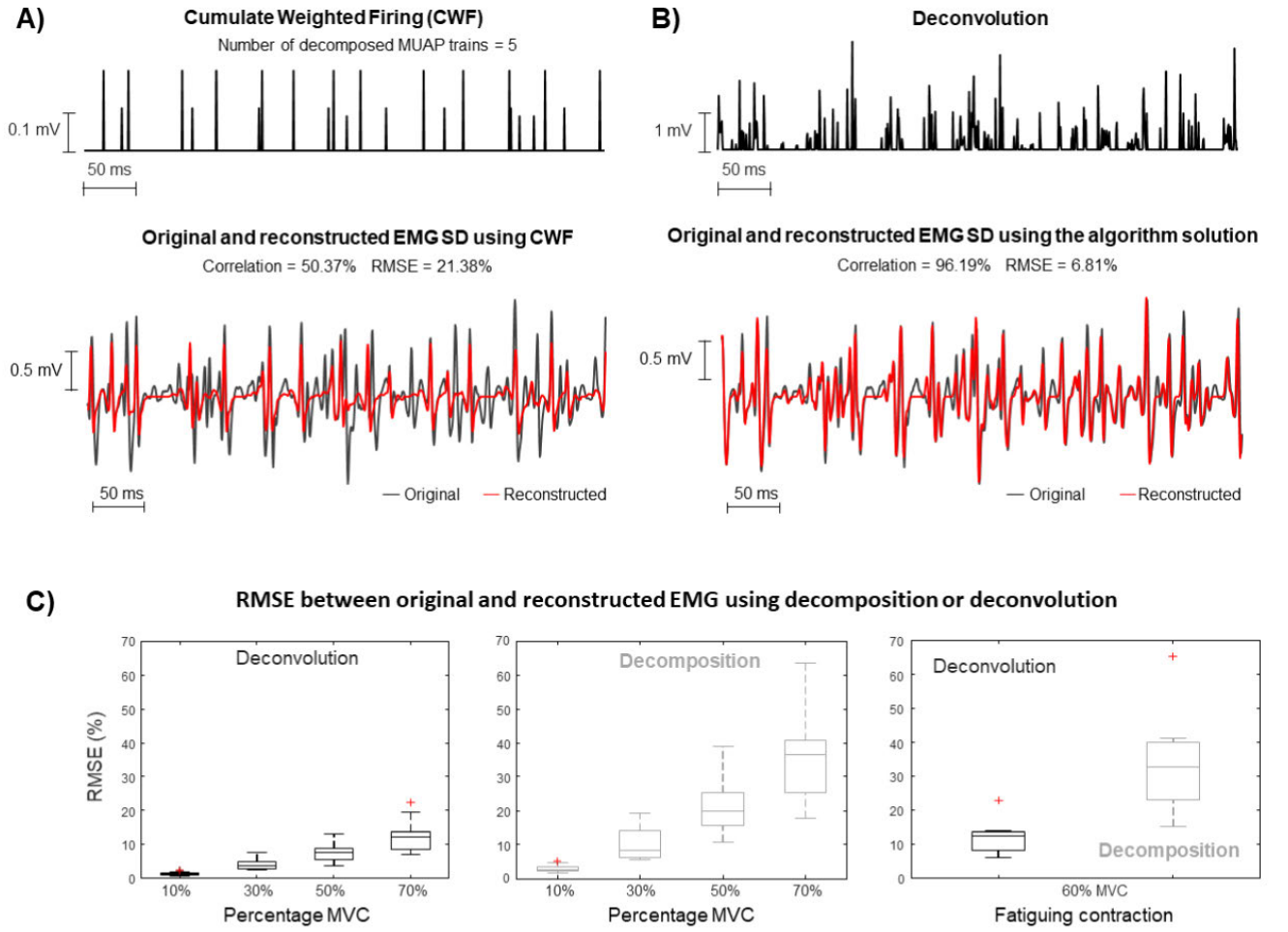

FIGURE 8. Decomposition of high-density EMG vs deconvolution. A) Example of CWF obtained as the sum of the firing trains of 5 MUs identified by decomposition and reconstruction of the processed signal as sum of MUAP trains. B) Same example signal as in A), but processed by deconvolution. C) Box and whiskers plots of the entire datasets (indicating median, quartiles, outliers and range, obtained after removing outliers) showing the distributions of root mean squared error (RMSE) between EMG and reconstruction obtained by either decomposition or deconvolution (single SD channel manually selected for each recording, IED of 8 mm).

than deconvolution (Figure 8). These results, together with the reliability of deconvolution in managing data with large interference rebuilt from many decomposed MUAP trains (Figure 7), suggest that the lower correlation with CWF from decomposition of original than reconstructed signals is in part due to the additional information accounted for by deconvolution.

Additional future work is suggested to evaluate this interesting indication. In fact, our results should be interpreted with caution, keeping in mind the limitations of our study. Deconvolution (like most processing methods) relies on an interpretive model and the extent to which it is accurately fitted is reflected in the goodness of the estimates provided. In essence, the underlying model considers the EMG as the sum of biphasic waveforms (i.e., the MUAPs) with similar shapes, but with arbitrary amplitudes and times of appearance. If these hypotheses are met with good accuracy, deconvolution can estimate the kernel (approximating the shape of MUAPs) and give the EMG as the convolution of this kernel with the estimated CWF (representing the amplitudes and the time onsets of the different MUAP contributions). To fit the hypotheses of deconvolution approach, we recorded data from a muscle with parallel fibers and the bipolar signals were extracted from positions beyond the most distal IZ. However, there are more complicated conditions (e.g., tissue inhomogeneity, pinnate muscles, multiple IZs, bipolar signals placed over the IZ, etc.) in which deconvolution cannot provide reliable results (but in those cases even the interpretation of the bipolar signal would be difficult). An extension of deconvolution to accommodate a few kernels (instead of a single one) has been proposed [41] (experimental validation is still needed, but promising results in simulations have been obtained). However, still experimental signals may deviate greatly from simplifying modelling assumptions, so that caution in the interpretation is always recommended.

Future works are suggested to further evaluate the accuracy and usefulness of our innovative method. For example, an indirect validation could be to use the estimated cumulative

spike trains as indicators of muscle activity for downstream applications, e.g., for joint angle regression and gesture classification.

V. CONCLUSION

Deconvolution of bipolar surface EMG is a low-cost method, both in terms of acquisition (requiring a single channel) and processing (which can be achieved in real time). Comparison tests with high-density EMG decomposition indicate that it provides reliable information on MU activity. Further validation is recommended in the future, e.g., by also considering intramuscular EMG as a reference. However, our results already clearly indicate that it is a promising method for many application fields (including ergonomics, sports science, clinics, myoelectric control), where information on MU behavior is very important, but simple and reliable acquisitions are required.

REFERENCES

[1] T. J. Herda, J. A. Siedlik, M. A. Trevino, M. A. Cooper, and J. P. Weir, "Motor unit control strategies of endurance-versus resistance-trained individuals," *Muscle Nerve*, vol. 52, no. 5, pp. 832–843, Nov. 2015.

[2] J. Basmajian and C. J. De Luca, *Muscles Alive: Their Function Revealed by Electromyography*, 5th ed. Baltimore, MD, USA: Williams & Wilkins, 1985.

[3] P. Contessa, A. Adam, and C. J. De Luca, "Motor unit control and force fluctuation during fatigue," *J. Appl. Physiol.*, vol. 107, no. 1, pp. 235–243, Jul. 2009.

[4] E. Martinez-Valdes, F. Negro, D. Falla, J. L. Dideriksen, C. J. Heckman, and D. Farina, "Inability to increase the neural drive to muscle is associated with task failure during submaximal contractions," *J. Neurophysiol.*, vol. 124, no. 4, pp. 1110–1121, Oct. 2020.

[5] E. Martinez-Valdes, F. Negro, D. Farina, and D. Falla, "Divergent response of low-versus high-threshold motor units to experimental muscle pain," *J. Physiol.*, vol. 598, no. 11, pp. 2093–2108, Jun. 2020.

[6] X. Hu, A. K. Suresh, W. Z. Rymer, and N. L. Suresh, "Altered motor unit discharge patterns in paretic muscles of stroke survivors assessed using surface electromyography," *J. Neural Eng.*, vol. 13, no. 4, Aug. 2016, Art. no. 046025.

[7] A. Van Boxtel and L. R. B. Schomaker, "Motor unit firing rate during static contraction indicated by the surface EMG power spectrum," *IEEE Trans. Biomed. Eng.*, vol. BME-30, no. 9, pp. 601–609, Sep. 1983.

[8] P. J. Lago and N. B. Jones, "Low-frequency spectral analysis of the e.m.g.," *Med. Biol. Eng. Comput.*, vol. 19, no. 6, pp. 779–782, 1981.

[9] O. P. Neto and E. A. Christou, "Rectification of the EMG signal impairs the identification of oscillatory input to the muscle," *J. Neurophysiol.*, vol. 103, no. 2, pp. 1093–1103, Feb. 2010.

[10] L. Mesin, "Non-propagating components of surface electromyogram reflect motor unit firing rates," *IEEE Access*, vol. 7, pp. 106155–106161, 2019.

[11] B. A. Conway, D. M. Halliday, S. F. Farmer, U. Shahani, P. Maas, A. I. Weir, and J. R. Rosenberg, "Synchronization between motor cortex and spinal motoneuronal pool during the performance of a maintained motor task in man," *J. Physiol.*, vol. 489, no. 3, pp. 917–924, Dec. 1995.

[12] C. Deluca and Z. Erim, "Common drive of motor units in regulation of muscle force," *Trends Neurosci.*, vol. 17, no. 7, pp. 299–305, 1994.

[13] D. Farina and F. Negro, "Common synaptic input to motor neurons, motor unit synchronization, and force control," *Exerc. Sport Sci. Rev.*, vol. 43, no. 1, pp. 23–33, 2015.

[14] S. N. Baker, J. M. Kilner, E. M. Pinches, and R. N. Lemon, "The role of synchrony and oscillations in the motor output," *Exp. Brain Res.*, vol. 128, nos. 1–2, pp. 109–117, Sep. 1999.

[15] C. M. Laine, E. Martinez-Valdes, D. Falla, F. Mayer, and D. Farina, "Motor neuron pools of synergistic thigh muscles share most of their synaptic input," *J. Neurosci.*, vol. 35, no. 35, pp. 12207–12216, Sep. 2015.

[16] C. J. De Luca and Z. Erim, "Common drive in motor units of a synergistic muscle pair," *J. Neurophysiol.*, vol. 87, no. 4, pp. 2200–2204, Apr. 2002.

[17] F. Hug, A. Del Vecchio, S. Avrillon, D. Farina, and K. Tucker, "Muscles from the same muscle group do not necessarily share common drive: Evidence from the human triceps surae," *J. Appl. Physiol.*, vol. 130, no. 2, pp. 342–354, Feb. 2021.

[18] D. Farina, R. Merletti, and R. M. Enoka, "The extraction of neural strategies from the surface EMG: An update," *J. Appl. Physiol.*, vol. 117, no. 11, pp. 1215–1230, Dec. 2014.

[19] R. M. Enoka and J. Duchateau, "Rate coding and the control of muscle force," *Cold Spring Harbor Perspect. Med.*, vol. 7, no. 10, Oct. 2017, Art. no. a029702.

[20] X. Zhang, G. Zhu, M. Chen, X. Chen, X. Chen, and P. Zhou, "Muscle force estimation based on neural drive information from individual motor units," *IEEE Trans. Neural Syst. Rehabil. Eng.*, vol. 28, no. 12, pp. 3148–3157, Dec. 2020.

[21] A. Del Vecchio, F. Negro, A. Holobar, A. Casolo, J. P. Folland, F. Felici, and D. Farina, "You are as fast as your motor neurons: Speed of recruitment and maximal discharge of motor neurons determine the maximal rate of force development in humans," *J. Physiol.*, vol. 597, no. 9, pp. 2445–2456, May 2019.

[22] C. Dai and X. Hu, "Finger joint angle estimation based on motoneuron discharge activities," *IEEE J. Biomed. Health Informat.*, vol. 24, no. 3, pp. 760–767, Mar. 2020.

[23] T. Kapelner, F. Negro, O. C. Aszmann, and D. Farina, "Decoding motor unit activity from forearm muscles: Perspectives for myoelectric control," *IEEE Trans. Neural Syst. Rehabil. Eng.*, vol. 26, no. 1, pp. 244–251, Jan. 2018.

[24] C. Chen, G. Chai, W. Guo, X. Sheng, D. Farina, and X. Zhu, "Prediction of finger kinematics from discharge timings of motor units: Implications for intuitive control of myoelectric prostheses," *J. Neural Eng.*, vol. 16, no. 2, Apr. 2019, Art. no. 026005.

[25] C. Chen, Y. Yu, X. Sheng, D. Farina, and X. Zhu, "Simultaneous and proportional control of wrist and hand movements by decoding motor unit discharges in real time," *J. Neural Eng.*, vol. 18, no. 5, Oct. 2021, Art. no. 056010.

[26] I. Mendez, D. Barsakcioglu, I. Vujaklija, D. Wetmore, and D. Farina, "Non-invasive real-time access to the output of the spinal cord via a wrist wearable interface," *BioRxiv*, 2021. [Online]. Available: https://www.biorxiv.org/content/10.1101/2021.04.06.438640v1

[27] H. Parsaei, D. W. Stashuk, S. Rasheed, C. Farkas, and A. Hamilton-Wright, "Intramuscular EMG signal decomposition," *Crit. Rev. Biomed. Eng.*, vol. 38, no. 5, pp. 435–465, 2010.

[28] R. M. Enoka, "Physiological validation of the decomposition of surface EMG signals," *J. Electromyogr. Kinesiol.*, vol. 46, pp. 70–83, Jun. 2019.

[29] C. J. De Luca, A. Adam, R. Wotiz, L. D. Gilmore, and S. H. Nawab, "Decomposition of surface EMG signals," *J. Neurophysiol.*, vol. 96, no. 3, pp. 1646–1657, Sep. 2006.

[30] A. Holobar and D. Zazula, "Gradient convolution kernel compensation applied to surface electromyograms," in *Proc. ICA*, in Lecture Notes in Computer Science, 4666, pp. 617–624.

[31] A. Holobar and D. Zazula, "Multichannel blind source separation using convolution kernel compensation," *IEEE Trans. Signal Process.*, vol. 55, no. 9, pp. 4487–4496, Sep. 2007.

[32] A. Gallina et al., "Consensus for experimental design in electromyography (CEDE) project: High-density surface electromyography matrix," *J. Electromyogr. Kinesiol.*, vol. 64, Jun. 2022, Art. no. 102656.

[33] I. Campanini, A. Merlo, C. Disselhorst-Klug, L. Mesin, S. Muceli, and R. Merletti, "Fundamental concepts of bipolar and high-density surface EMG understanding and teaching for clinical, occupational, and sport applications: Origin, detection, and main errors," *Sensors*, vol. 22, no. 11, p. 4150, May 2022.

[34] M. Gazzoni, B. Afsharipour, and R. Merletti, "Surface EMG in ergonomics and occupational medicine," *Surf. Electromyogr., Physiol., Eng., Appl.*, vol. 31, pp. 361–391, 2016.

[35] A. D. Vigotsky, I. Halperin, G. J. Lehman, G. S. Trajano, and T. M. Vieira, "Interpreting signal amplitudes in surface electromyography studies in sport and rehabilitation sciences," *Frontiers Physiol.*, vol. 8, p. 985, Jan. 2018.

[36] G. I. Papagiannis, A. I. Triantafyllou, I. M. Roumpelakis, F. Zampeli, P. G. Eleni, P. Koulouvaris, E. C. Papadopoulos, P. J. Papagelopoulos, and G. C. Babis, "Methodology of surface electromyography in gait analysis: Review of the literature," *J. Med. Eng. Technol.*, vol. 43, no. 1, pp. 59–65, Jan. 2019.

[37] I. Campanini, C. Disselhorst-Klug, W. Z. Rymer, and R. Merletti, "Surface EMG in clinical assessment and neurorehabilitation: Barriers limiting its use," *Frontiers Neurol.*, vol. 11, p. 934, Sep. 2020.
[38] L. J. Myers, M. Lowery, M. O'Malley, C. L. Vaughan, C. Heneghan, A. S. C. Gibson, Y. X. R. Harley, and R. Sreenivasan, "Rectification and non-linear pre-processing of EMG signals for cortico-muscular analysis," *J. Neurosci. Methods*, vol. 124, no. 2, pp. 157–165, Apr. 2003.
[39] L. Mesin, "Separation of interference surface electromyogram into propagating and non-propagating components," *Biomed. Signal Process. Control*, vol. 52, pp. 238–247, Jul. 2019.
[40] L. Mesin, "Single channel surface electromyogram deconvolution to explore motor unit discharges," *Med. Biol. Eng. Comput.*, vol. 57, no. 9, pp. 2045–2054, Sep. 2019.
[41] L. Mesin, "Motor unit discharges from multi-kernel deconvolution of single channel surface electromyogram," *Electronics*, vol. 10, no. 16, p. 2022, Aug. 2021.
[42] M. Bourges, G. R. Naik, and L. Mesin, "Single channel surface electromyogram deconvolution is a useful pre-processing for myoelectric control," *IEEE Trans. Biomed. Eng.*, vol. 69, no. 5, pp. 1767–1775, May 2022.
[43] A. Holobar, M. A. Minetto, and D. Farina, "Accurate identification of motor unit discharge patterns from high-density surface EMG and validation with a novel signal-based performance metric," *J. Neural Eng.*, vol. 11, no. 1, Feb. 2014, Art. no. 016008.
[44] A. Holobar, V. Glaser, J. A. Gallego, J. L. Dideriksen, and D. Farina, "Non-invasive characterization of motor unit behaviour in pathological tremor," *J. Neural Eng.*, vol. 9, no. 5, Oct. 2012, Art. no. 056011.
[45] T. M. M. Vieira, I. D. Loram, S. Muceli, R. Merletti, and D. Farina, "Postural activation of the human medial gastrocnemius muscle: Are the muscle units spatially localised?" *J. Physiol.*, vol. 589, no. 2, pp. 431–443, Jan. 2011.
[46] K. E. Power, E. J. Lockyer, A. Botter, T. Vieira, and D. C. Button, "Endurance-exercise training adaptations in spinal motoneurones: Potential functional relevance to locomotor output and assessment in humans," *Eur. J. Appl. Physiol.*, vol. 122, no. 6, pp. 1367–1381, Jun. 2022.
[47] H. Reucher, J. Silny, and G. Rau, "Spatial filtering of noninvasive multielectrode EMG: Part II-filter performance in theory and modeling," *IEEE Trans. Biomed. Eng.*, vol. BME-34, no. 2, pp. 106–113, Feb. 1987.
[48] C. S. Burrus. *Iterative Reweighted Least Squares*. Accessed: Mar. 20, 2024. [Online]. Available: https://anilkeshwani.github.io/files/iterative-reweighted-least-squares-12.pdf
[49] L. Mesin and D. Cocito, "A new method for the estimation of motor nerve conduction block," *Clin. Neurophysiol.*, vol. 118, no. 4, pp. 730–740, Apr. 2007.
[50] L. Mesin, E. Lingua, and D. Cocito, "Motor nerve conduction block estimation in demyelinating neuropathies by deconvolution," *Bioengineering*, vol. 9, no. 1, p. 23, Jan. 2022.
[51] D. Craven, B. McGinley, L. Kilmartin, M. Glavin, and E. Jones, "Compressed sensing for bioelectric signals: A review," *IEEE J. Biomed. Health Informat.*, vol. 19, no. 2, pp. 529–540, Mar. 2015.
[52] L. Mesin, D. Dardanello, A. Rainoldi, and G. Boccia, "Motor unit firing rates and synchronisation affect the fractal dimension of simulated surface electromyogram during isometric/isotonic contraction of vastus lateralis muscle," *Med. Eng. Phys.*, vol. 38, no. 12, pp. 1530–1533, Dec. 2016.
[53] S. Muceli, W. Poppendieck, A. Holobar, S. Gandevia, D. Liebetanz, and D. Farina, "Blind identification of the spinal cord output in humans with high-density electrode arrays implanted in muscles," *Sci. Adv.*, vol. 8, no. 46, Nov. 2022, Art. no. eabo5040.
[54] S. H. Nawab, S.-S. Chang, and C. J. De Luca, "High-yield decomposition of surface EMG signals," *Clin. Neurophysiol.*, vol. 121, no. 10, pp. 1602–1615, Oct. 2010.
[55] M. Shinohara, K. G. Keenan, and R. M. Enoka, "Contralateral activity in a homologous hand muscle during voluntary contractions is greater in old adults," *J. Appl. Physiol.*, vol. 94, no. 3, pp. 966–974, Mar. 2003.

LUCA MESIN received the degree in electronics engineering, in 1999, and the Ph.D. degree in applied mathematics from Politecnico di Torino, Italy, in 2003. He is currently an Associate Professor of biomedical engineering and a Supervisor of the Mathematical Biology and Physiology Group, Department of Electronics and Telecommunications, Politecnico di Torino. His current research interests include biomedical image and signal processing and mathematical modeling.

EMILIANO ROBERT received the master's degree in biomedical engineering from Politecnico di Torino, Italy, in 2022. His master's thesis was on the experimental validation of the deconvolution of EMG.

GENNARO BOCCIA received the master's degree in advanced sciences of sport training from the University of Turin, Italy. His Ph.D. study was focused on methodological aspects of EMG to study muscle fatigue and muscle coordination. He was a Research Fellow with the University of Verona and a Visiting Researcher with the University of Birmingham. He is currently a Researcher with the University of Turin. He is investigating the effects of muscle fatigue on muscle contraction quickness and on physical performances that rely on such a physical capacity. He has adopted the means of high-density surface electromyography to non-invasively monitor the motor units' properties and the spatial distribution of electromyographic activity across the muscle.

TAIAN VIEIRA was born in Rio de Janeiro, Brazil, in 1980. He received the degree in motor sciences and the M.Sc. degree in biomedical engineering from Universidade Federal do Rio de Janeiro, in 2005 and 2007, respectively, and the Ph.D. degree in biomedical engineering from Politecnico di Torino, in 2011. From September 2011 to August 2016, he was an Associate Professor with Universidade Federal do Rio de Janeiro. He is currently an Assistant Professor with Politecnico di Torino. He has coauthored three book chapters and over 80 articles. His research interests include muscle neurophysiology, posture control, EMG-biofeedback, and electrical stimulation applied to healthy and disabled subjects. In 2008, he received the Student Presentation Award from the International Society of Electrophysiology and Kinesiology and was the Inaugural Winner of the Emerging Scientist Award of the International Society of Biomechanics, in 2011. He received the Doctoral Scholarship provided by the Brazilian Research Council for the Ph.D. degree.

Open Access funding provided by 'Politecnico di Torino' within the CRUI CARE Agreement